

QUIET SUN MAGNETIC FIELDS FROM SPACE-BORNE OBSERVATIONS: SIMULATING HINODE'S CASE

D. OROZCO SUÁREZ, L.R. BELLOT RUBIO, AND J.C. DEL TORO INIESTA

Instituto de Astrofísica de Andalucía (CSIC), Apdo. 3004, 18080 Granada, Spain; orozco@iaa.es, lbellot@iaa.es, jti@iaa.es

Accepted in ApJ Letters

ABSTRACT

We examine whether or not it is possible to derive the field strength distribution of quiet Sun internetwork regions from very high spatial resolution polarimetric observations in the visible. In particular, we consider the case of the spectropolarimeter attached to the Solar Optical Telescope aboard Hinode. Radiative magneto-convection simulations are used to synthesize the four Stokes profiles of the Fe I 630.2 nm lines. Once the profiles are degraded to a spatial resolution of $0''.32$ and added noise, we infer the atmospheric parameters by means of Milne-Eddington inversions. The comparison of the derived values with the real ones indicates that the visible lines yield correct internetwork field strengths and magnetic fluxes, with uncertainties smaller than ~ 150 G, when a stray light contamination factor is included in the inversion. Contrary to the results of ground-based observations at $1''$, weak fields are retrieved wherever the field is weak in the simulation.

Subject headings: Sun: magnetic fields – Sun: photosphere – Instrumentation: high angular resolution

1. INTRODUCTION

The characterization of quiet sun internetwork (IN) fields is an important issue in solar physics. Polarimetric measurements of the visible Fe I lines at 630.2 nm and the near-infrared Fe I lines at 1565 nm have been used to advance our knowledge of IN magnetism, but no consensus has been reached yet. While the analysis of the visible lines suggest a predominance of kG field strengths and small filling factors (Sánchez Almeida & Lites 2000; Domínguez Cerdeña et al. 2003; Socas-Navarro & Lites 2004), the near-infrared lines indicate that most fields have hG strengths with larger filling factors (Lin 1995; Lin & Rimele 1999; Khomenko et al. 2003; Martínez González et al. 2006; Domínguez Cerdeña et al. 2006).

Attempts to reconcile these contradictory results have argued that visible and IR lines sample different magnetic structures in the resolution element (Sánchez Almeida & Lites 2000; Socas-Navarro & Sánchez Almeida 2003) or that noise affects the visible lines more dramatically than the IR lines (Bellot Rubio & Collados 2003). On the other hand, Martínez González et al. (2006) have convincingly demonstrated that it is not possible to obtain reliable IN field strengths from the Fe I 630.2 nm lines due to crosstalk with thermodynamical parameters at $1''$ resolution.

Different techniques have been proposed to study IN fields, but the diagnostic potential of high spatial resolution observations in the absence of atmospheric seeing has only been explored by Khomenko et al. (2004). The spectropolarimeter (SP; Lites et al. 2001) of the Solar Optical Telescope (SOT) aboard Hinode (Ichimoto et al. 2005) is already providing nearly diffraction-limited observations of the solar photosphere, and upcoming instruments will do so in the future (e.g., IMAx aboard SUNRISE or VIM aboard Solar Orbiter). Thus, there is a clear need to assess whether reliable IN field strengths can be derived from space-borne observations.

Here we address this question by simulating and analyzing Hinode/SP measurements. Radiative magneto-convection simulations are used to synthesize the Stokes profiles of the Fe I 630.2 nm lines. The profiles are

degraded to the nearly diffraction-limited resolution of $0''.32$ achieved by Hinode/SP. After adding noise to the Stokes spectra, the atmospheric parameters are inferred by means of inversion techniques. By comparing the derived values with the real ones we determine the errors in field strength and magnetic flux to be expected from the analysis of Hinode data. Our main result is that Milne-Eddington (ME) inversions of the visible 630.2 nm lines yield correct IN field strengths with uncertainties smaller than 150 G for the whole range of strengths from ~ 0.1 to 1 kG. If internetwork fields are hG fields, then simple ME inversions of Hinode/SP measurements will result in sub-kG field strength distributions, contrary to what is obtained from current ground-based observations.

2. MHD SIMULATIONS, SPECTRAL SYNTHESIS, AND IMAGE DEGRADATION

To describe the sun in the more realistic way possible we use radiative MHD simulations by Vögler et al. (2005). Specifically, we take three snapshots from different simulation runs representing very quiet, unipolar internetwork and network regions with average unsigned fluxes of 10, 50, and 200 Mx cm⁻², respectively. The horizontal and vertical extents of the computational box are 6 and 1.4 Mm. The synthesis of the Stokes spectra of the two Fe I lines is carried out using the SIR code (Ruiz Cobo & del Toro Iniesta 1992). The spectral region is sampled at 113 wavelength positions in steps of 2.15 pm, following the Hinode/SP normal map mode (for details, see Shimizu 2004). The atomic parameters have been taken from the VALD database (Piskunov et al. 1995).

The aperture of Hinode/SOT is 0.5 m, which operating at 630 nm provides a spatial resolution of $\sim 0''.26$ (equivalent to ~ 190 km on the solar surface). The sampling interval in the MHD simulations is $0''.0287$, implying a spatial resolution of $0''.057$ (41.6 km). Thus, in order to simulate SOT observations, the synthetic Stokes profiles derived from the MHD model have been spatially degraded by telescope diffraction. In addition, we have considered the extra loss of contrast caused by the integration of the signal in the detector. Finally, the images

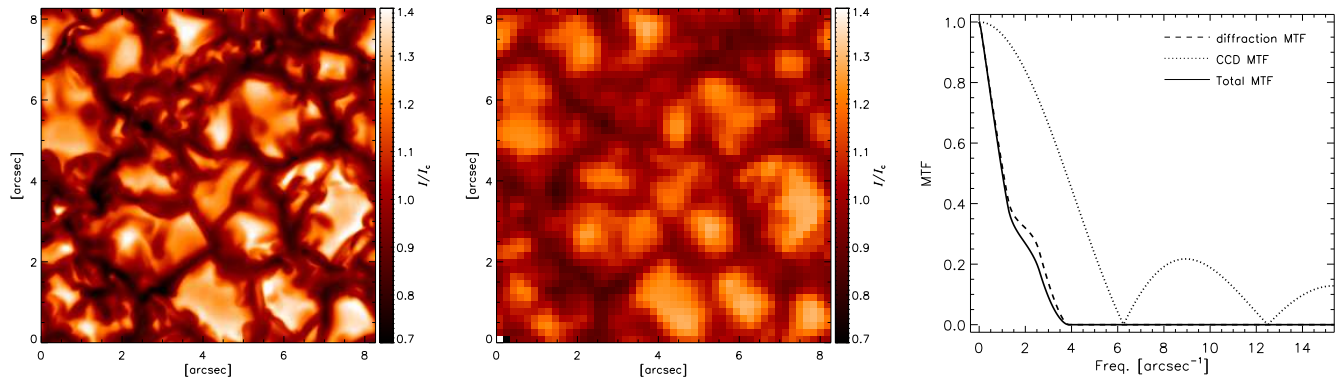


FIG. 1.— *Left and middle:* Continuum intensity maps for the simulation snapshot with average unsigned flux of 10 Mx cm^{-2} and for the data spatially degraded considering telescope diffraction and pixel size. Color scales are the same in the two maps. The contrast varies from 13.7% in the original image to 8.5% in the degraded one. *Right:* MTF of the detector (dotted line), diffraction limited MTF (dashed line), and combination of both effects (solid line).

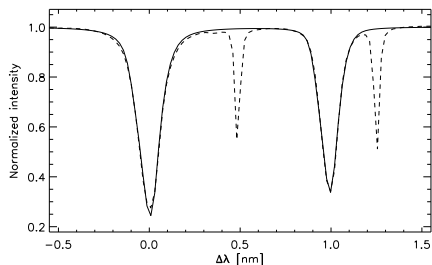


FIG. 2.— Comparison between the average Stokes I profile from the spatially degraded data (solid) and the FTS spectral atlas (dashed). Both continua are normalized to unity.

are rebinned to the SP CCD pixel size of $0''.16 \times 0''.16$. Figure 1 shows continuum intensity maps for the original and the spatially degraded data. The degradation process reduces the rms contrast from $\sim 14\%$ to $\sim 9\%$ in the continuum. The pixelation of the CCD is noticeable in the degraded image. The right panel of Fig. 1 shows Modulation Transfer Functions (MTFs) describing the filtering of spectral components induced by telescope diffraction and pixelation effects in the CCD. Note the modification of the effective MTF caused by the central obscuration of the entrance pupil.

Figure 2 compares the average Stokes I profiles from the spatially degraded data and the NSO Fourier Transform Spectrometer Atlas of the quiet Sun. Both spectra are very similar, with only small differences in the line core and wings of Fe I 630.1 nm. Note that the lack of a temporal average exclude, for instance, the effect of the 5-min oscillation in the simulated profile. To reproduce an Hinode/SP observation we have also convolved the profiles with a Gaussian of 30 mÅ FWHM to account for the spectral resolving power of the spectrograph and have added noise at the level of 10^{-3} of the continuum intensity I_c (the polarimetric sensitivity of standard Hinode/SP measurements).

3. INVERSION

To derive the magnetic field strength from the simulated profiles we use a least-square inversion technique based on ME atmospheres. ME inversions represent the best option to interpret the measurements if one is not interested in vertical gradients of the physical quantities. They are simple and often provide reasonable averages of the atmospheric parameters over the line formation re-

gion (Westendorp Plaza et al. 2001; Bellot Rubio 2006).

We apply the ME inversion to the Fe I 630.15 nm and Fe I 630.25 nm lines simultaneously. A total of 9 free parameters are determined (S_0 , S_1 , η_0 , $\Delta\lambda_D$, a , B , γ , χ , and v_{LOS} ; for the meaning of the symbols see, e.g., Orozco Suárez & del Toro Iniesta 2007). No additional broadening of the profiles by macroturbulence or microturbulence is allowed. Three different inversions are performed to derive the atmospheric parameters. All of them use a simple one-component model, i.e., a laterally homogeneous magnetic atmosphere occupying the whole resolution element. We first invert the profiles in the absence of noise, and then with noise added at the level of $10^{-3} I_c$. In the last inversion, the noisy profiles are fitted considering non-zero stray light contaminations factors. The stray light profile is evaluated individually for each pixel by averaging the Stokes I profiles within a box $1''$ -wide centered on the pixel. For all inversions we use the same initial guess model, allowing a maximum of 300 iterations. The initial field strength is 100 G.

4. RESULTS

Figure 3 shows the vector magnetic field (strength, inclination, and azimuth) retrieved from the inversions of the Stokes profiles. The first column displays a cut of the simulation snapshot with average flux density of 10 Mx cm^{-2} at optical depth $\log \tau = -2$. The second and third columns contain the results of the ME inversions of the spatially degraded profiles in the absence of noise and the specific case of a SNR of 1000, respectively. Finally, the fourth column shows the atmospheric parameters derived from the noisy profiles accounting for stray light contamination. White regions represent pixels which have not been inverted because of their small polarization signals (we only consider pixels whose Stokes Q , U or V amplitudes exceed three times the noise level).

Over the granules, the magnetic field strength is very weak and the polarization signals are buried in the noise. These pixels represent $\sim 55\%$ of the total area (white regions in Fig. 3). The stronger fields concentrate in intergranular regions. In those regions, the magnetic structures inferred from the inversion have bigger sizes than the real ones, i.e., they appear “blurred”. This is caused by the degradation of the images due to telescope diffraction and CCD pixel size. The field inclination and azimuth structures resulting from the inversion are blurred

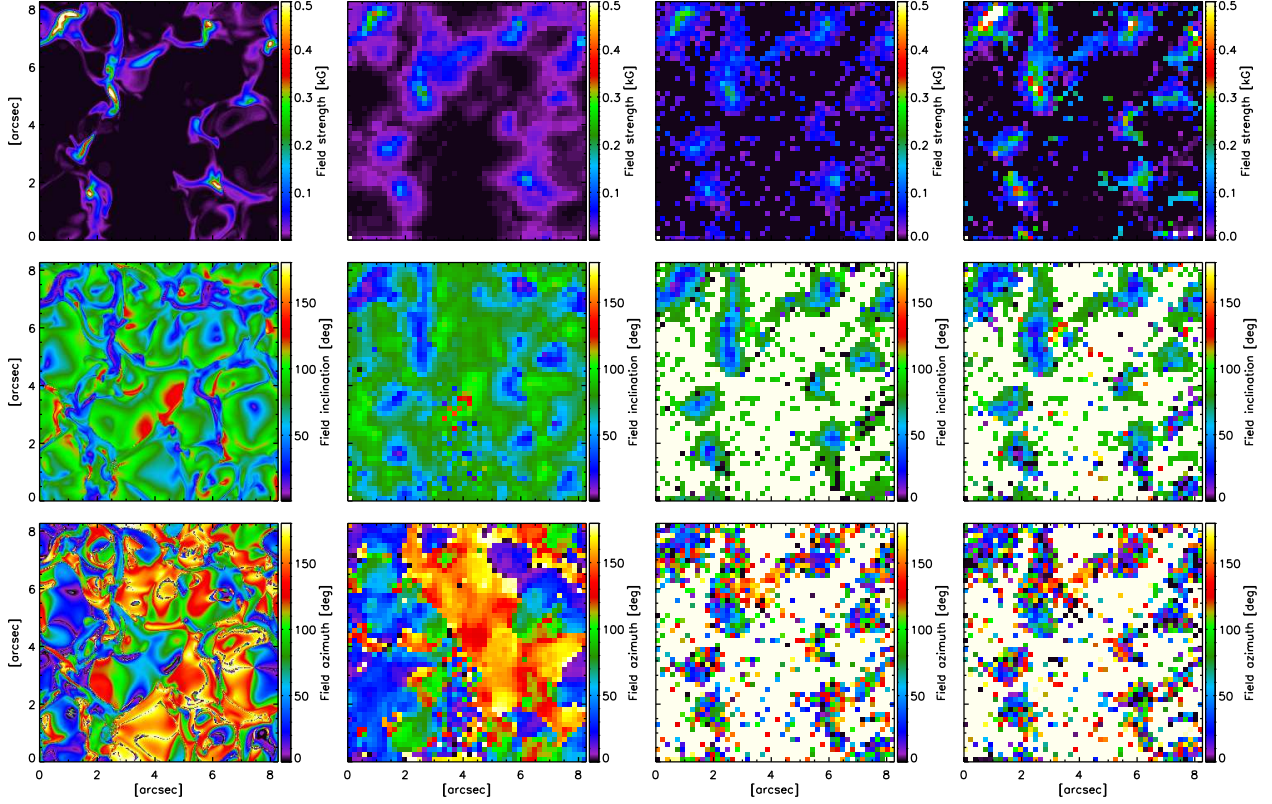


FIG. 3.— *Left:* Cuts at optical depth $\log \tau = -2$ of the model atmospheres provided by the MHD simulation with averaged unsigned flux of 10 Mx cm^{-2} . *Second column:* Maps of the physical quantities retrieved from the ME inversion of the profiles with no noise. *Third column:* Maps retrieved from the ME inversion of the profiles with SNR of 1000 and no stray light contamination. *Fourth column:* Same as before, but accounting for stray light. From top to bottom: magnetic field strength, inclination, and azimuth.

as well. The azimuth values are rather uncertain because of the tiny linear polarization signals produced by the weak fields of the simulations.

Figure 4 is a close up of small features observed in intergranular regions. Note that each Hinode/SP pixel of $0''.16 \times 0''.16$ corresponds to 36 pixels in the simulation, hence they usually contain a broad distribution of magnetic field strengths. When we consider that the polarization signal is produced by a single magnetic component within the resolution element and no stray light is allowed for, the inferred field strengths are smaller than those in the model, so the field is underestimated (middle panels of Fig. 4). If one accounts for stray light contamination the inferred fields become stronger (right panels), but also noisier due to the increased number of free parameters.

To analyze the results in a more quantitative way we calculate the mean and rms values of the errors. We define the error as the difference between the inferred and the real parameters at optical depth $\log \tau = -2$. Since one pixel of the degraded data corresponds to 36 pixels in the simulations, we compare each inverted pixel with the mean of the corresponding 36 pixels in the original map. Figure 5 shows the mean and rms errors of the field strength resulting from the inversion without accounting for stray light (top left panel). It is clear that fields above $\sim 100 \text{ G}$ are underestimated, with rms errors smaller than $\sim 150 \text{ G}$ in the whole range of strengths. The results are similar for the magnetic flux density (top right panel). The inversion considering stray light contamination yields much better inferences, as can be seen

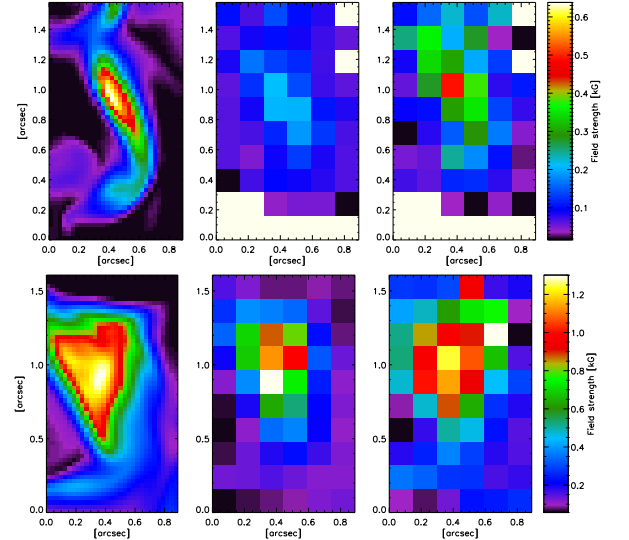


FIG. 4.— *Left:* Field strengths at $\log \tau = -2$ in the MHD simulations with 10 Mx cm^{-2} (top) and 50 Mx cm^{-2} (bottom). *Middle:* Field strengths derived from the ME inversion of the spatially degraded Stokes profiles with SNR 1000 and no stray light contamination. *Right:* Field strengths from the ME inversion accounting for stray light contamination.

in the bottom panels of Fig. 5. The field strength and flux are slightly overestimated for weak fields, but the rms errors do not exceed 150 G in any case.

5. DISCUSSION

Previous analyses of visible (630.2 nm) and near-infrared (1565 nm) neutral iron lines do not agree on

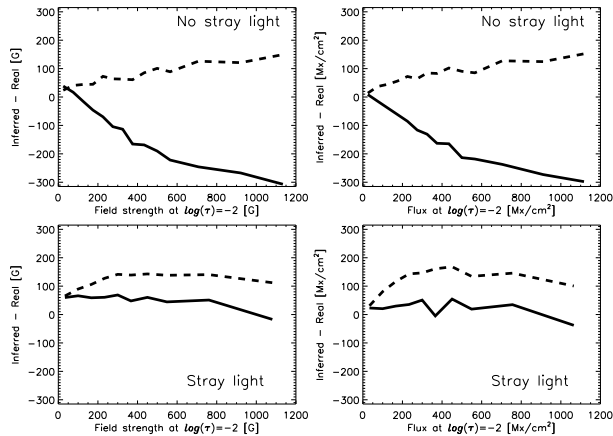


FIG. 5.— *Top*: Mean (solid) and rms (dashed) errors of the field strength (left) and flux (right) derived from the inversion of the profiles with SNR=1000 assuming a single magnetic atmosphere and no stray light contamination. *Bottom*: Same as before but accounting for stray light contamination.

the distribution of field strengths in IN regions. In particular, the visible lines systematically deliver kG field strengths and small filling factors, while the near-infrared lines suggest a predominance of hG fields.

Here we have shown that ME inversions of the Fe I 630 nm lines at spatial resolutions of $0''.32$ (the case of Hinode/SP) underestimate the magnetic field strength by some hundred G if no stray light contamination is included. When stray light is accounted for, ME inversions are able to recover any magnetic field above 100 G with remarkable accuracy.

Interestingly, we always derive weak fields from the simulated Hinode/SP observations where the field in the MHD model is weak. Likewise, pixels assigned strong fields by the ME inversion actually correspond to strong fields in the MHD model. This is in sharp contrast with the results of Martínez González et al. (2006), who always infer kG fields from the Fe I 630.2 nm lines observed in the IN at resolutions of $1''$ – $1''.5$ when the inversion is initialized with strong fields. The difference is probably due to: (a) our significantly higher spatial resolution, which narrows the range of field strengths present in the pixel; (b) the fact that we do not employ two-component atmospheres, micro- or macro-turbulent velocities, which

reduces the degrees of freedom of the solution; and (c) the simple description of the thermodynamics provided by the ME model which, contrary to the atmosphere used by Martínez González et al. (2006), does not allow to compensate for incorrect magnetic parameters. On the other hand, our results seem to contradict the conclusions of Bellot Rubio & Collados (2003). However, the signals considered here are larger by a factor of ~ 10 due to the much higher angular resolution (which implies larger filling factors). Under these conditions, noise does not significantly affect the field strengths derived from the visible lines (see Fig. 5 in Bellot Rubio & Collados 2003).

We caution that the results of this Letter may only be valid as long as the MHD simulations provide a realistic description of the Sun. The performance of ME inversions could be different if the magnetic field is structured on scales much smaller than $\sim 0''.3$. For the moment, however, there is no compelling evidence that tiny magnetic elements exist in the quiet solar photosphere.

6. CONCLUSIONS

Our analysis suggests that Hinode/SP observations will make it possible to determine the real distribution of field strengths in quiet Sun internetwork regions. Simple one-component Milne-Eddington inversions without macro and microturbulence seem appropriate to achieve that goal. However, it will be essential to account for the degradation of the image induced by telescope diffraction and detector pixel size. The work presented here shows that the effects of the degradation can be modeled sufficiently well including a stray light contamination factor in the inversion.

We thank A. Vögler and M. Schüssler for making their MHD simulations available and answering our questions about them. The program used to degrade the synthetic Stokes profiles was written by J.A. Bonet and S. Vargas. This work has been partially funded by the Spanish Ministerio de Educación y Ciencia through project ESP2003-07735-C04-03 (including European FEDER funds) and *Programa Ramón y Cajal*.

REFERENCES

- Bellot Rubio, L. R. 2006, ASP Conf. Ser.: Solar Polarization 4, 358, 107
- Bellot Rubio, L. R., & Collados, M. 2003, A&A, 406, 357
- Domínguez Cerdeña, I., Kneer, F., & Sánchez Almeida, J. 2003, ApJ, 582, L55
- Domínguez Cerdeña, I., Almeida, J. S., & Kneer, F. 2006, ApJ, 646, 1421
- Ichimoto, K., & Solar-B Team 2005, Journal of Korean Astronomical Society, 38, 307
- Khomenko, E. V., Collados, M., Solanki, S. K., Lagg, A., & Trujillo Bueno, J. 2003, A&A, 408, 1115
- Khomenko, E., Collados, M., & Solanki, S.K. 2004, Mem. S.A. It., 75, 282
- Lin, H. 1995, ApJ, 446, 421
- Lin, H., & Rimmele, T. 1999, ApJ, 514, 448
- Lites, B. W., Elmore, D. F., & Stander, K. V. 2001, ASP Conf. Ser.: Advanced Solar Polarimetry – Theory, Observation, and Instrumentation, 236, 33
- Martínez González, M.J., Collados, M., & Ruiz Cobo, B. 2006, A&A, 456, 1159
- Orozco Suárez, D., & del Toro Iniesta, J.C. 2007, A&A, 462, 1137
- Piskunov, N. E., Kupka, F., Ryabchikova, T. A., Weiss, W. W., & Jeffery, C. S. 1995, A&A Supp. Ser., 112, 525
- Ruiz Cobo, B., & del Toro Iniesta, J. C. 1992, ApJ, 398, 375
- Sánchez Almeida, J., & Lites, B.W. 2000, ApJ, 532, 1215
- Shimizu, T. 2004, ASP Conf. Ser.: The Solar-B Mission and the Forefront of Solar Physics, 325, 3
- Socas-Navarro, H., & Sánchez Almeida, J. 2003, ApJ, 593, 581
- Socas-Navarro, H., & Lites, B.W. 2004, ApJ, 616, 587
- Vögler, A., Shelyag, S., Schüssler, M., Cattaneo, F., Emonet, T., & Linde, T. 2005, A&A, 429, 335
- Westendorp Plaza, C., del Toro Iniesta, J.C., Ruiz Cobo, B., Martínez Pillet, V., Lites, B.W., & Skumanich, A. 2001, ApJ, 547, 1130